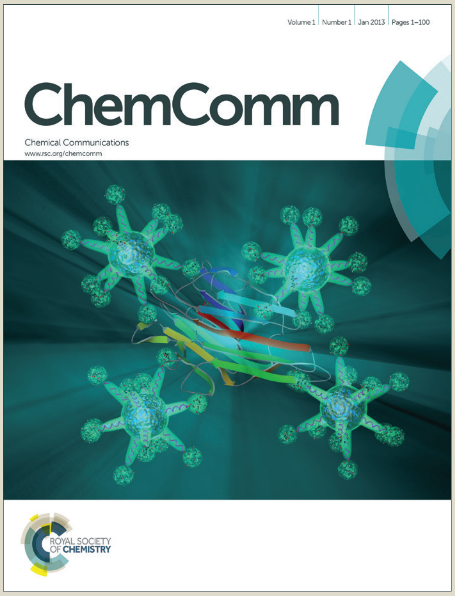
Volume 1 | Number 1 | Jan 2013 | Pages 1–100
ChemComm
Chemical Communications
www.rsc.org/chemcomm
ROYAL SOCIETY OF CHEMISTRY

Journal Name

ChemComm

Dynamic Article Links ►

Cite this: DOI: 10.1039/c0xx00000x

www.rsc.org/xxxxxx

ARTICLE TYPE

Assorted morphosynthesis: Access to multi-faceted nano-architectures from a super-responsive dual π-functional amphiphilic construct

Deepak Asthana, Jyoti Shukla, Srikanta Dana, Varsha Rani, Ajayakumar M. R., Kamla Rawat, Kalyanashis Mandal, Premlata Yadav, Subhasis Ghosh, and Pritam Mukhopadhyay*

Received (in XXX, XXX) Xth XXXXXXXXX 20XX, Accepted Xth XXXXXXXXX 20XX
DOI: 10.1039/b000000x

An electronically segmented amphiphile was created by conjugating two π-functional units Hydroxyquinoline and Naphthalenediimide (HQ/NDI) for the first time. Differential electrostatic potential of the π-surfaces, H-bonding units, etc. trigger manifold response and directs a unique collection of seven diverse nano-architectures. Chiral assembly, distinct classes of fibers, 3-D sheets, metallo-spheres/fibrils with μM levels of Co/Cu/Zn (II) ions emerged from this new approach of assorted morphosynthesis under ambient condition.

There has been a tremendous interest to synthesize diverse nano-architectures from functional organic/inorganic systems for applications in opto-electronics, nano-sensors and magnetic materials.[1-2] Till date, from a single amphiphile it has been possible to generate primarily two types of nano-structures e.g. micelles/vesicles and fibers/sheets.[3] Similarly, amphiphiles generating charge-transfer-based assemblies and the supra-amphiphiles are also restricted to only two types of distinct morphologies.[4] Although there has been great advances in the area of responsive amphiphiles,[3a,b] it remains a great design and synthetic challenge to accomplish multiple nano-architectures with different aspect-ratios, dimensions and periodicity from a single amphiphilic entity.

To evolve such a rare assemblage, hydroxyquinoline (HQ) and naphthalenediimide (NDI) units were integrated for the first time which bestow differential electronic π-surfaces in the amphiphile (Scheme 1). This special design with HQ as the electron-rich polar head-group, complementary H-bonding groups, metal ion chelation ability and electron-deficient NDI π-surface provide unprecedented responsiveness. Importantly, seven distinct forms of nano-architectures was generated mostly in mixed-aqueous solution and strictly under ambient conditions (Scheme 2). Chiral assembly, 3-D sheets, tunable fiber classes and assembled metallo-spheres/fibrils generated with μM levels of Co/Zn/Cu (II) ions are the emergent features of this new approach of assorted morphosynthesis. These assemblies were also probed on different surfaces and examined through different microscopic techniques to confirm the robustness of the nano-/micro- architectures.

Computational studies were in agreement with our prognosis of an electronically segmented amphiphile, since the electrostatic surface potential (ESP) differential of the HQ and NDI moiety was clearly evident (See SI: figure S1). Also, the HOMO and LUMO was localized on the electron-rich HQ and the electron-deficient NDI moiety, respectively (Scheme 1b).[5] In addition to the differential ESP's, we anticipated that the H-bonding groups of the HQ unit should bestow ability in the amphiphile to sense and divergently respond to small changes in the polarity of the medium.

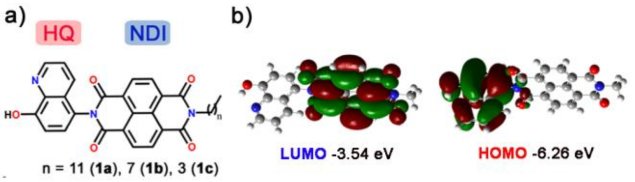

Scheme 1 a) Molecular structure of **1a-c**; b) Localization of the LUMO and HOMO surface on the NDI and the HQ moiety, respectively.

The metal ion chelation ability of the HQ unit and the large π-surfaces of the amphiphile would provide high degree of responsiveness to a variety of stimuli to achieve a controlled and distinct assortment of nano-architectures.

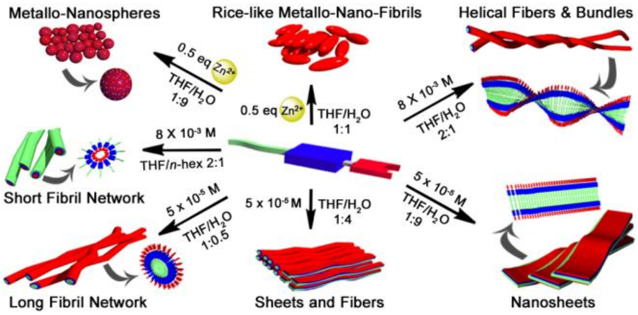

Scheme 2 Assortment of nano-architectures obtained from **1a** under ambient conditions in a controlled and precise manner.

The HQ moiety is of prime attraction due to its organic light emitting diode (OLED) properties,[6a] as a modulator in neurodegenerative disorders,[6b] as sensors[6c] and phosphorent organogels.[6d] Likewise, the NDI moiety[7a,b] has found wide-ranging applications e.g. *n*-type semiconduction,[7c] anion-π catalysis,[8] donor-acceptor assemblies,[9] DNA binding,[10] electron transfer (ET) reactions,[11a] multi-stable systems,[11b] ultra-electron deficient systems and stable radical ions.[12] To our knowledge, the handful of amphiphiles known till date with individual units of the HQ or NDI have allowed only the generation of fiber/vesicle-based architectures.[13]

The amphiphiles **1a**, **1b** and **1c** were synthesized by the condensation of 1,4,5,8-napthalenetetracarboxylic dianhydride with 5-amino-8-hydroxyquinoline and the respective aliphatic amines e.g. dodecyl, octyl and butyl amine, respectively. The molecules were characterized by various analytical methods (See SI). **1a** was found to self-assemble in a large window of polarity e.g. in mixed aqueous solutions and also in nonpolar solvents. In contrast, **1b** and **1c** with shorter alkyl tails had solubility constraints in these wide-ranging solvent medium. Therefore, hydrophilic-lipophilic(H-L) balance[14] was key to achieve responsive self-assembly. To ensure reproducibility, the synthesis of each class of nano-architectures were repeated at least 4-5 times.

In a mixed aqueous solution of THF/H_2O (1:0.5 v/v) **1a** formed ultra-long fibers of several micro-meters in length as determined by TEM studies (Figure 1a). Width of the thinnest fiber was found to be ~5.8 nm, which is in agreement with the twice of the molecular length ~2.76 nm of **1a** determined from computational studies (See SI). Gradual increment in the proportion of water to 1:4 (v/v) drastically modulated the self-assembly pattern and initiated the formation of nano-sheets (See SI: figures S2). The co-existence of the fibrillar structures along with the nano-sheets can be clearly seen in Figure 1b. On further increment of water to 1:9 (v/v) the fibers completely reorganized to form micro-meter long 3-D sheets (Figure 1c-d) (See SI: figure S3).

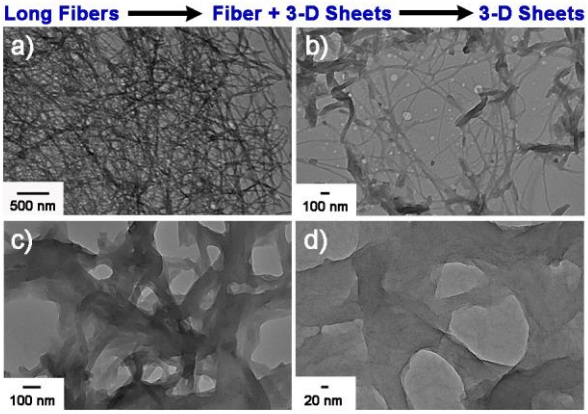

Fig. 1 TEM images of **1a** (5×10^{-5} M): (a) THF/H_2O (1:0.5 v/v) showing long fibers, (b) THF/H_2O (1:4 v/v) showing fiber to sheet transformation, (c) THF/H_2O (1:9 v/v) showing complete transformation into 3-D sheets, and (d) 3-D multi-layered sheets.

Interestingly, at a significantly higher concentration of 0.5 wt% and THF/H_2O ratio of 1:0.5 (v/v) the self-assembly characteristics of **1a** was further modulated and chiral organization was discerned. Long helical fibers organized into multiple helical bundles were observed. High resolution TEM images showed that the helical fibers had pitch length of upto ~60 nm (Figure 2a-d) (See SI: figure S4). Such macroscopic chiral organization from an achiral amphiphile is highly attractive and possibly results from the stacking interactions of the two orthogonally oriented π-functional scaffolds.

On the other hand, by increasing the lipophilicity, **1a** at 0.5 wt% in THF/*n*-Hexane (1:0.5 v/v) formed ultra-short fibrillar structures of 100-300 nm in length and devoid of any helical twisting (Figure 2e-f). Therefore, in the presence of a lipophilic medium extent of self-organization gets highly limited due to lack of adequate hydophobic forces in comparison to that achieved in hydrophilic medium.

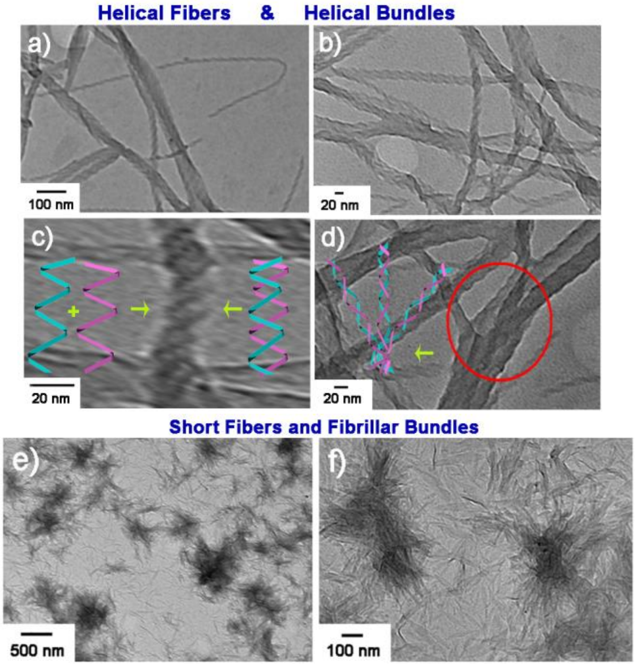

Fig. 2 TEM images of **1a**; (a) to (d) depicting the long helical bundles in THF/H_2O, 1:0.5 (v/v), 0.5 wt%, (e) and (f) short fibers and fibrillar bundles in THF/n-Hexane, 1:0.5 (v/v), 0.5 wt%.

Nextly, we evaluated the ability of **1a** to morphologically respond to metal ions. In the presence of alkali/alkaline earth metal ions the original sheet-like structures of **1a** in THF/H_2O (1:9 v/v) did not show any changes. However, **1a** readily responded to 0.5 equiv. of Zn (II) ions and formed interconnected nanosphere-like structures (Figure 3). These structures varied from 100-250 nm in diameter and formed extended stacks of nanospheres (See SI: figure S5).

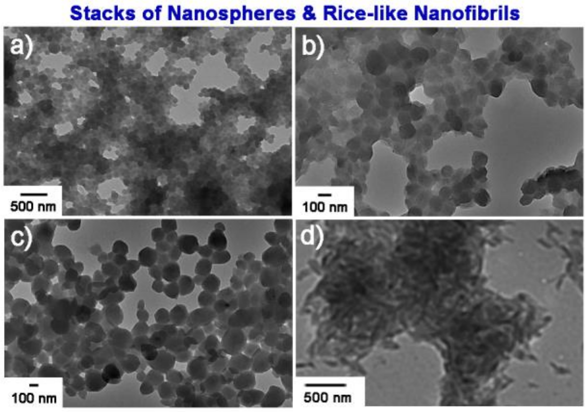

Fig. 3 TEM images of (a)-(c) self-assembled stacks of nanospheres and (d) rice-like nanofibrils. **1a** (5×10^{-5} M) with 0.5 equiv. of Zn (II), (a)-(c): in 1:9 THF/H_2O (v/v) and (d) in 1:1 THF/H_2O (v/v).

Likewise, Co/Cu (II) ions with **1a** showed similar structures (See SI: figures S6-S7). Interestingly, **1a** in the presence of only 0.05 equiv. of Zn/Co/Cu (II) ions showed the initiation of the nanospheres within the predominant sheet-like stuctures. Therefore, **1a** can respond to Zn (II) ions and form nanospheres even at 5-25 μM levels. Remarkably, we found that by increasing the lipophilicity to THF/H$_2$O 1:1 (v/v) **1a** with 0.5 equiv. of Zn (II) ions formed ultra-short rice-like metallo-fibrils of 100-200 nm in length (see SI: figure S8).

The ability of **1a** to sequester transition metals at μM levels and transform into new nano-architectures provides attractive platform for nano-sensing and imaging. Energy dispersive X-ray (EDX) coupled with TEM imaging[15]showed distributed Zn (II) ions in the nanospheres (Figures 4a-c).

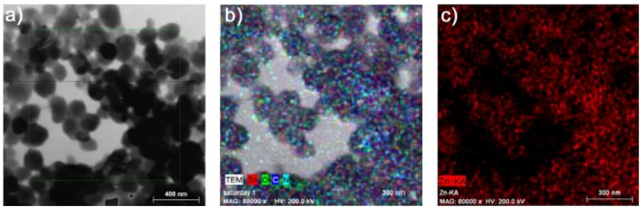

Fig. 4 (a) TEM images and (b-c) EDX mapping of the elements in the nanospheres with 0.5 equiv. of Zn (II) ions in 1:9 THF/H$_2$O (v/v).

Likewise, presence of Co (II) ions in the assembled nanospheres was confirmed (See SI: figures S9-S10). These assembled nanospheres also exhibited strong emission when equilibrated with fluorescein dye as revealed by CLSM studies (See SI: figure S11). Metallo-nanospheres with organic amphiphiles are rare and was recently demonstrated with polymers in the presence of Ca/Ba (II) ions.[16]

It is to be noted that there is a possibility of biased formation of self-assembled structures dependent on the surface of study. In all the above cases of TEM based imaging, the nano-/micro-architectures were studied on a holey carbon film attached to a meshed Cu-grid. To explore the effect of other surfaces on the self-assembled structures we studied the diverse morphologies on quartz/*p*-type Si surfaces. As a representative example we studied a particular type of self-assembled structure on quartz and Si surface by optcial microscopy. Ultra-long fibers of several micrometers were formed on both of these surfaces (see SI: figure S12). Nextly, the morphologies formed under different conditions on these surfaces were systematically studied by atomic force microscopy (AFM). The long fibers, combination of fibers and sheets and the 3-D sheets formed on the quartz surface were clearly observed by AFM imaging (Figures 5a-c).

At higher concentrations of 0.5 wt% in THF/H$_2$O inter-twined helical fibrillar bundles could be discerned (Figure 5d). On the other hand, in THF/*n*-hexane, short fibrillar structures were clearly seen (Figure 5e). In the presence of Zn(II) ions, AFM imaging clearly demonstrated interconnected nanosphere-like structures on the quartz surface (Figure 5f). These set of control experiments confirmed the versatility of the amphiphile to form similar nano-/micro-architectures on different surfaces and also points to the robustness of this self-assembly process.

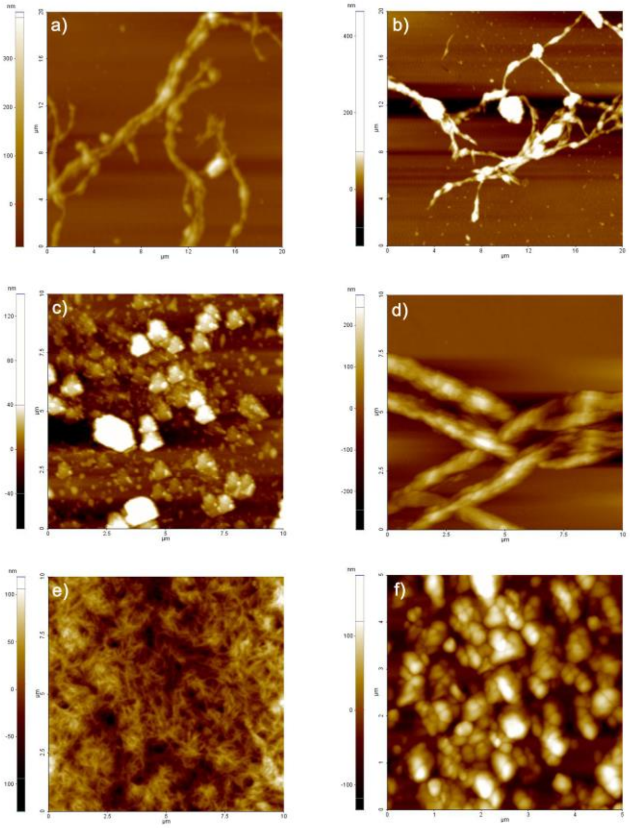

Fig. 5 AFM images of **1a** showing (a) long fibers, (b) fiber to sheet transformation, (c) 3-D sheets, (d) long helical bundles, (e) short fibers and (f) stacks of nanospheres.

Furthermore, we evaluated the opto-electronic properties of **1a** under conditions of self-assembly. It was found from Differential Pulse Voltammetry (DPV) that the reduction potential of the NDI moiety in the nano-architectures can be suitably tuned with varied amounts of water. Thus, **1a** showed a large second reduction potential compression from (–) 1.21 V in THF to (–) 0.80 V in THF:H$_2$O (1:1) with small changes in the first reduction potential (See SI: Table 1 and figure S13). The optical absorption properties of **1a** was also modulated with increased polarity of the medium (See SI: figures S14). Thus with increasing amounts of water the π-π^* transition of NDI at 355 and 375 nm was red-shifted by 10 nm and broadening of peaks were observed. Therefore, self-assembly clearly tunes the opto-electronic properties of **1a**.

To have an insight into the molecular forces that drive the self-assembly process we performed UV-Vis, NMR, FT-IR, spectroscopy and electrochemical studies. UV-Vis studies of **1a** with increasing amounts of water established that the hydrophobic forces direct the aggregation of the NDI scaffold as evident from the red-shift of its signature absorption bands. In addition, the stabilization of the π-scaffolds in the assemblies by increased amounts of water was clear from the lowering of the NDIs second reduction potential by 400 mV. Since majority of the assemblies were studied at ~10^{-5} M meaningful information could not be extracted for these assemblies from the NMR experiments. For the self-assembly process in 0.5 wt% (THF-d_8:D$_2$O) the ^{1}H NMR and 2-D NOESY experiments remained inconclusive due to severe broadening of peaks (See SI: figure S15).

We then performed FT-IR studies of representative assemblies on Si surface in the reflection mode. Significant changes in the asymmteric stretching frequency of the imide carbonyl groups of the NDI scaffold, C=N/C-N stretching frequency of the HQ scaffold and the C-H stretching frequencies of the alkyl chain were observed in the assembly of the helical bundles formed at 0.5 wt% in THF/H_2O (1:0.5 v/v) compared to the smaller fibers at 0.5 wt% in THF/*n*-Hexane (1:0.5 v/v) (see SI: figure S16). For example, in the helcial bundles the hydrophobic forces play a key role in the assembly process and lowering of the asymmetric stretching frequency of the imide carbonyl group of the NDI scaffold by 19 cm^{-1}, and C=N/C-N stretching frequencies of the HQ scaffold by 6/9 cm^{-1} compared to the assembly of the smaller fibers. Also a considerable broadening of the C-H stretching frequencies were observed in the helical bundles. From these experiments it is clear that hydrophobic forces play a major role in the self-assembly process and the π-functional NDI-HQ scaffolds along with the alkyl chain contributes to different extent in the formation of the nano-/micro architectures. We believe that due to the limitations of the conventional spectroscopic techniques in studying assemblies in dilute solutions, single molecule spectroscopic methods would be able to throw better light on understanding and differentiating the molecular interactions in the nano-/micro-architectures.[17]

The generation of these diverse collection of nano-structures is due to the interplay of several intricate factors: a) H-bonding groups on the HQ and NDI unit makes it super-responsive to minute changes in the polarity of solvent, b) H-L balance offered by the amphiphile affords a large window of solubility in mixed-aqueous as well as nonpolar solutions, c) differential ESP of the π-surfaces ingrain explicit information to control the hydrphobic forces and d) metal ion chelation ability of the amphiphile. Ability to orthogonally transduce this information let us achieve nano-structures having wide control over shape, periodicity and dimension ranging from few nm to tens of μm.

In conclusion, a new electronically segmented amphiphilic design is presented providing for the first time an easy access to a unique collection of seven diverse nano-architectures. Importantly, these nano-structures were generated in mixed aquous solution and under ambient condition avoiding the common stimuli like heat and light. Control experiments of the nano-/micro-architectures on different surfaces established that the self-assembly process is quite robust. We believe imparting such super-responsiveness in the molecule and ability to manifest multiplicity in orthogonal fashion provides intriguing possibilities to harness novel biological, chemical and material function from a single amphiphilic entity.

We thank DBT-BUILDER, DST-FIST for the funding and AIRF, JNU, New Delhi for the instrumentation facilities.

Notes and references

Supramolecular and Material Chemistry Lab, School of Physical Sciences, Jawaharlal Nehru University, New Delhi 110 06, India.
Fax: (+91) 11-2674 2891; Tel: (+91) 11-2673 8772;
E-mail: m_pritam@mail.jnu.ac.in

† For the synthesis, characterization, electron microscopy images, UV-Vis and fluorescence spectra, electrochemical data and computational studies see Electronic Supplementary Information (ESI): See DOI: 10.1039/b000000x/

1 (a) E. Climent, M. D. Marcos, R. Martínez-Máñez, F. Sancenón, J. Soto, K. Rurack and P. Amorós, *Angew. Chem. Int. Ed.* 2009, **48**, 8519; (b) R. Kaminker, R. P.-Biro, M. E. van der Boom, *Angew. Chem. Int. Ed*. 2011, **50**, 3224; (c) L. Meazza, J. A. Foster, K. Fucke, P. Metrangolo, G. Resnati, J. W. Steed, *Nature Chem*. 2013, **5**, 42; (d) M. Perrier, M. Busson, G. Massasso, J. Long, V. Boudousq, J. -P. Pouget, S. Peyrottes, Ch. Perigaud, C. Porredon-Guarch, J. de Lapuente, M. Borras, J. Larionova and Y. Guari, *Nanoscale*, 2014, **6**, 13425; (e)S. Shankar, R. Balgley, M. Lahav, S. R. Cohen, R. P.-Biro and M. E. van der Boom, *J. Am. Chem. Soc*., 2015, **137**, 226.

2 (a) E. Dujardin and S. Mann, *Adv. Mater*., 2004, **16**, 1125; (b) M. Mas-Torrent, C. Rovira and J. Veciana, *Adv. Mater*., 2013, **25**, 462; (c) M. Mas-Torrent, N. Crivillers, C. Rovira, J. Veciana, *Chem. Rev*. 2012, **112**, 2506.

3 (a) H.-J. Kim, T. Kim and M. Lee, *Acc. Chem. Res*., 2011, **44**, 72; (b) A. Sorrenti, O. Illa and R. M. Ortuno, *Chem. Soc. Rev*., 2013, **42**, 8200.

4 (a) Y. J. Jeon, P. K. Bharadwaj, S. Choi, J. W. Lee and K. Kim, *Angew. Chem. Int. Ed*. 2002, **41**, 4474; (b) C. Wang, Y. Guo, Y. Wang, H. Xu, R. Wang and X. Zhang, *Angew. Chem. Int. Ed*. 2009, **47**, 8962 (c) X. Chi, X. Ji, D. Xia, and F. Huang, *J. Am. Chem. Soc*., 2015, **137**, 1440.

5 M. J. Frisch, *et al*., Gaussian 09W, Rev: D.01, Gaussian Inc., Wallingford, CT, 2009. Pl. refer to the SI for the complete reference.

6 (a) C. W. Tang, S. A. Van Slyke, *Appl. Phys. Lett.*, 1987, **51**, 913; (b) M. A. Greenough, J. Camakaris, A. I. Bush, *Neurochem. Int*. 2013, **62**, 540; (c) S. Sarkar and R. Shunmugam, *Chem. Commun*. 2014, **50**, 8511; (d) M. Shirakawa, N. Fujita, T. Tani, K. Kaneko, M. Ojima, A. Fujii, M. Ozaki and S. Shinkai, *Chem. Eur. J*. 2007, **13**, 4155.

7 (a) S. -L. Suraru and F. Würthner, *Angew. Chem. Int. Ed*. 2014, **53**, 7428; (b) N. Sakai, J. Mareda, E. Vauthey and S. Matile, *Chem. Commun.*, 2010, **46**, 4225; (c) H. E. Katz, A. J. J. Lovinger, Johnson, C. Kloc, T. Seigrist, W. Li, Y.-Y. Lin, A. Dodabalapur, *Nature*, 2000, **404**, 478.

8 (a) V. Gorteau, G. Bollot, J. Mareda, A. Perez-Velasco, and S. Matile *J. Am. Chem. Soc*., 2006, **128**, 14788; (b) Y. Zhao, Y. Domoto, E. Orentas, C. Beuchat, D. Emery, J. Mareda, N. Sakai and S. Matile, *Angew. Chem. Int. Ed*. 2013, **52**, 9940.

9 (a) H. Y. Au-Yeung, F. B. L. Cougnon, S. Otto, G. D. Pantoş and J. K. M. Sanders, *Chem. Sci*., 2010, **1**, 567; (b) M. R. Molla, A. Das and S. Ghosh, *Chem. Eur. J*. 2010, **16**, 10084.

10 A. R. Smith and B. L. Iverson, *J. Am. Chem. Soc*., 2013, **135**, 12783.

11 (a) M. R. Ajayakumar, D. Asthana and P. Mukhopadhyay, *Org. Lett*. 2012, **14,** 4822; (b) M. R. Ajayakumar, G. Hundal and P. Mukhopadhyay, *Chem. Commun*., 2013, **49**, 7684.

12 S. Kumar, M. R. Ajayakumar, G. Hundal and P. Mukhopadhyay, *J. Am. Chem. Soc*., 2014, **136**, 12004.

13 (a) S. Basak, J. Nanda and A. Banerjee, *Chem. Commun*., 2013, **49**, 6891; (b) K. P. Nandre, S. V. Bhosale, K. V. S. Rama Krishna, A. Gupta and S. V. Bhosale, *Chem. Commun*., 2013, **49**, 5444.

14 R. W. Egan, M. A. Jones and A. L. Lehninger, *J. Biol. Chem.* 1976, **251**, 4442.

15 Energy Dispersive X-Ray Analysis in the Electron Microscope by D. C. Bell and A. J. -G. Reed, BIOS Scientific Publishers Limited, Oxford, UK, 2003.

16. F. Freire, J. M. Seco, E. Quiñoá, and R. Riguera, *J. Am. Chem. Soc*., 2012, **134**, 19374.

17. S. Sharma, N. Pal, P. K. Chowdhury, S. Sen, and A. K. Ganguli, *J. Am. Chem. Soc*., 2012, **134**, 19677.